JOURNAL GEOLOGICAL SOCIETY OF INDIA
Vol.97, March 2021, pp.255-260

New Finding of Silica-deficient Sapphirine-bearing Granulites from NNE of Suranganar Village, Southern Madurai Block, India

Swapnil Kumar Rai[a,*], Divya Prakash[a], Roopali Yadav[a], Srishti Jaiswal[a], R.S. Kumar[b] and Chandra Kant Singh[a]

[a] Centre of Advanced Study in Geology, Banaras Hindu University, Varanasi - 221 005, India
[b] Department of Earth Sciences, Annamalai University, Annamalai Nagar - 608 002, India
***E-mail:** ksrbhu5@gmail.com*

ABSTRACT

An infrequent occurrence of sapphirine from metapelite rocks of the Cardamom hills of South India has been reported. This report of sapphirine may not be the first from the Southern Granulite Terrane (SGT) but is essentially from a new locality. The studied metapelites are silica-undersaturated devoid of garnet and the sapphirine symplectites. The symplectites of orthopyroxene + cordierite, orthopyroxene + K-feldspar + cordierite, orthopyroxene + sapphirine + cordierite ± K-feldspar ± biotite, orthopyroxene + biotite + cordierite + K-feldspar are discernible. The textural patterns show partial to complete pseudomorphism of the initially formed orthopyroxene and sapphirine and their succeeding decomposition to present stage. The relative X_{Mg} calculated for the key minerals show the trend as: Crd > Spr > Bt > Opx. The pseudosection modelling and the calculated P-T diagram drawn from the average bulk composition of the studied metapelite connote isothermal decompression with peak pressure and temperature conditions stable at ~10 Kbar and ~985 °C respectively. The assemblage reported in this study has an important bearing on the crustal evolution of the high-grade metamorphism exhumed from a deeper level of the crust.

INTRODUCTION

Sapphirine with general cell formula $Mg_{16-n}Al_{32+2n}Si_{8-n}O_{80}$ (where n varies from 0 to 2.5) (Vogt, 1947) with slight departure noted in proposed n values (Deer et al., 1962) is a robust indicator of UHT-metamorphism (when in association with quartz). However, the preservation of sapphirine is rare because it usually breaks down to spinel + quartz (Moore, 1968), cordierite and K-feldspar (Kelsey and Hand, 2015) during decompression or retrograde cooling. There have been reports of sapphirine from the Southern Madurai Block (SMB hereafter) (Anto et al., 1998; Shazia et al., 2012), however, the aforementioned reports are indeterminate as they do not incorporate any specified location in terms of coordinates. Sapphirine being the first and the primitive member of the sapphirine supergroup of minerals is mostly associated with High-Temperature to Ultra-High-Temperature grade metamorphic rocks as well as it is also found in magmatic rocks. The associated arrested textures found in sapphirine granulites enable the extraction of P – T trajectories and hence provide insights to the deep crustal dynamic processes (Kelsey et al., 2006; Santosh and Sajeev, 2006; Mukhopadhyay and Basak, 2009; Prakash et al., 2019). In the current research, we are not just furnishing the textural and compositional facets of sapphirine and associated minerals from the metapelites recovered but also, we are bringing up a better understanding of the crustal evolution and the scenario of UHT – Metamorphism in the studied area. The textural implications give a direct handout and a focussed understanding of the sapphirine breakdown to its present symplectitic occurrence and its connection with other minerals within the rock. Also, the combined study of reaction textures, preserved metamorphic crystallization imprints and pseudosection modelling would highly resolve the crustal metamorphic evolution and related effective processes.

GEOLOGICAL FRAMEWORK

The Mg – Al rich metapelites bearing sapphirine and other compositions show heterogeneity in non-identical microspheres. The sampling was done along the cardamom hills, from nearly 4 km NNE of Suranganar village (9°39'21" N and 77°12'42" E) (Fig. 1). Geographically, Suranganar village is located near to the Kerala and Tamil Nadu border and the studied area geologically falls within the MB, southern India. Tectonically, the southern part of south India, dominated by granulite facie rocks is believed to have been accreted over the northern part of south India (the Archean granite-greenstones) and sutured along an oceanic suture, the Palghat – Cauvery Suture Zone (Santosh et al., 2009, 2011). The granulites from the southern part of South India are considered to be of the Proterozoic age and are impregnated with polymetamorphic histories (Raith et al., 1997; Santosh et al., 2003; Sajeev et al., 2006; Prakash et al., 2018). The sapphirine bearing metapelites show sporadic occurrences with no definite localisation pattern within the dominant lithology i.e. Orthopyroxene bearing granulites. However, at the regional scale, the encountered lithologies vary as, charnockites, garnet-cordierite gneiss, calc-silicates and two-pyroxene granulites. However, some carbonatite and syenite intrusions are quite apprehensible.

MESOSCOPIC FEATURES OF THE ROCK

The dominant lithology hosting the few and far between sapphirine – granulites are essentially charnockite, the latter shows the essential charnockitic composition and retrogressed charnockite (pyroxene to amphibole) assemblages. The sapphirine bearing patches show a very slight bluish hue preferably due to the presence of cordierite. The sample as a whole shows light and earthy colour, where biotite and feldspar are easily distinguishable, also, at some spots on the cut surface of the sample, green specks indicate presence of sapphirine (Fig. 2).

PETROGRAPHIC STUDIES AND METAMORPHIC REACTIONS

Detailed textural studies reveal the presence of Mg-Al silicate mineral, sapphirine, occurring as symplectites with cordierite as well as a fully engulfed or suspended mineral within cordierite matrix. The studied samples are devoid of garnet, sillimanite and

0016-7622/2021-97-3-255/$ 1.00 © GEOL. SOC. INDIA | DOI: 10.1007/s12594-021-1675-5

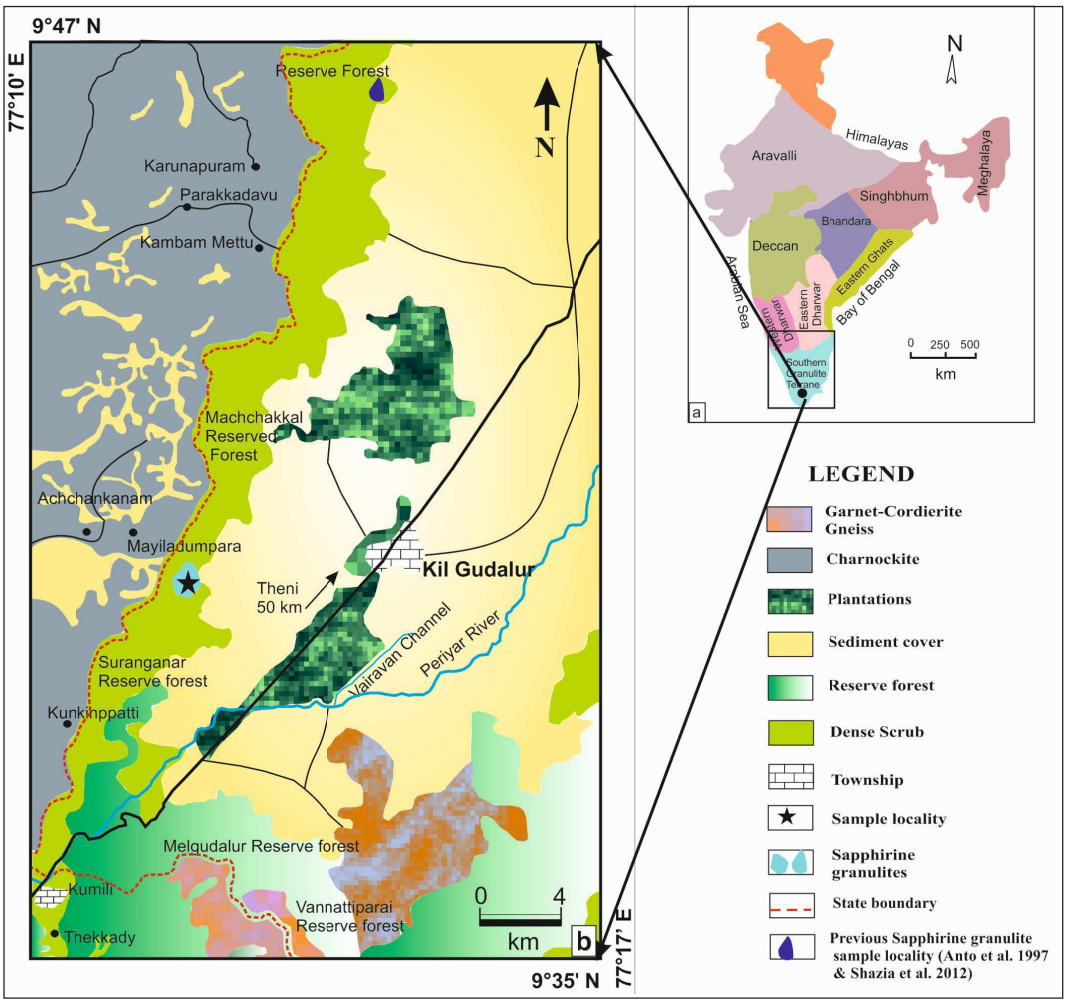

Fig.1. (a) Simplified map showing the position of the Southern Granulite Terrain (SGT) along with other adjacent cratons. **(b)** Geological map of the area around Gudalur.

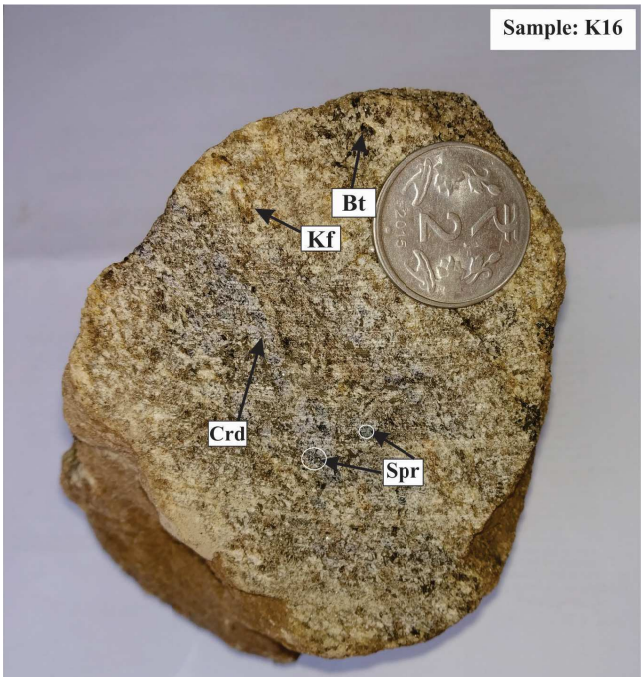

Fig.2. The studied sapphirine granulite from study area. Note the coarse-grained aggregates of sapphirine (Spr), cordierite (Crd), K-feldspar (Kf) and Biotite (Bt).

quartz thus, rendering them to be silica-undersaturated. The textural relation studies shows the existence of various stable mineral parageneses as:

P1 – Spr + Crd + Opx + Bt + Pl + Kfs,
P2 – Opx + Crd + Bt + Kfs ± Pl, and
P3 – Crd + Opx + Bt ± Kfs ± Pl

Apart from the aforementioned mineral phases, the other minor assemblages include zircon, monazite, ilmenite, rutile and apatite.

The typical symplectitic association of sapphirine and cordierite (Fig. 3a) in different domains within the same rock could be envisioned with textural differences at the grain size level. The Sapphirine – cordierite association essentially seems to be symplectitic but, this symplectite could be seen set in coarse grains of cordierite in which the sapphirine grains either are fully or partially surrounded by the former. The symplectitic domains are spread evenly throughout the rock sample and appear much to be like pods of sapphirine. The core of these pods is occupied by sapphirine – cordierite symplectites whereas the rim is occupied by cordierite. However, no other mineral except rutile could be found to be associated directly with sapphirine within these symplectites.

With the absence of quartz, spinel, garnet, corundum and sillimanite in the rock sample, deducing the metamorphic reaction responsible for the formation of such symplectites becomes complex

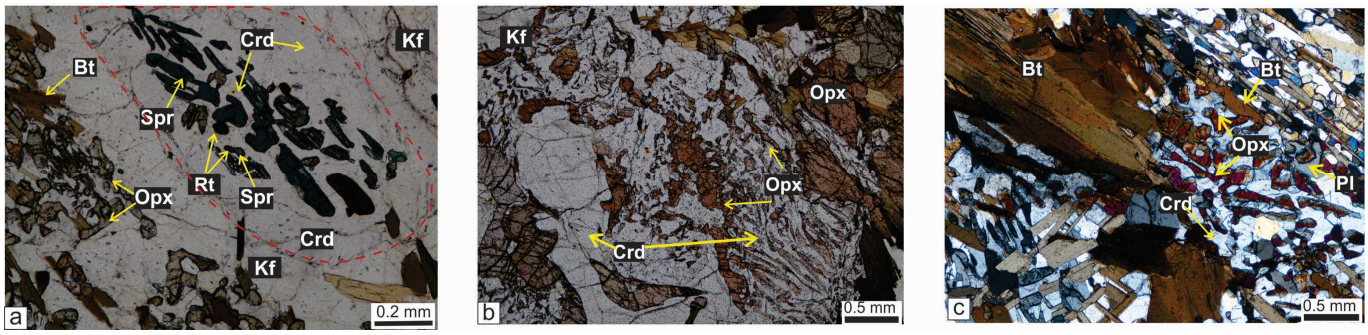

Fig.3. Photomicrographs illustrating textural relations in the sapphirine granulite: **(a)** symplectite of sapphirine and cordierite and contact of rutile and sapphirine (PL); **(b)** symplectitic intergrowth of orthopyroxene-cordierite (PL); **(c)** intergrowth of cordierite, orthopyroxene and biotite near coarse grained biotite (XL).

and interesting. However, the most plausible mechanism(s) that could be deciphered is two possible reactions as:

Reaction – 1:

$$Opx + Sil + Bt = Spr + Crd + Kfs \quad (R-1)$$

Alternatively, the above reaction may also proceed as:

Reaction – 2:

$$Sil + Opx = Spr + Crd \quad (R-2)$$

The above reaction could be possible only when presence of sillimanite (an Al-bearing phase) is being assumed in the rock body and with the progress in metamorphic conditions all the sillimanite gets fully consumed forming the aforementioned reaction products.

Reaction – 3:

The other considerable mechanism that could be the most probable outcome is the reaction between the Mg-rich orthopyroxene and Al-rich melt. However, the presumption of peraluminous melt (Al-rich melt) as an infiltrate during metamorphism, formed due to anatectic melting of Al-rich pelitic rocks from the surrounding area is the key to this reaction. The reaction could be summarised in the form of a reaction equation as:

$$Mg - Opx + Al - Melt = Spr + Crd + Melt \quad (R-3)$$

The above metamorphic reactions document silica – deficient conditions (Grew, 1984; Harley et al., 1990 & Raith et al., 1997). However, the assumptions and above reactions have also been discussed by Shazia et al., (2012), which show much similarity in case studies and the mineral assemblages encountered while carrying out the research.

Reaction – 4:

Other important mineral textures studied were the symplectites of orthopyroxene cordierite and biotite (Fig. 3b and c). Fine lamellae of Opx and Crd could be seen locally overgrowing biotite as symplectites. Biotite here gets resorbed by intergrowing Opx and Crd. However, a significant trail of pseudomorphed porphyroblastic garnet could be seen by the rimming of the platy biotite by Opx – Crd symplectite. Also, very late stage coarse-grained biotite could be seen (Fig. 3c) growing at the expense of orthopyroxene. This late stage retrograde mineral reaction could be summarised in the form of an equation as:

$$Bt + Plg \pm Q = Opx + Crd + Melt \quad (R-4)$$

Mineral Chemistry

The mineral chemistry was determined by the Electron Probe Micro Analyzer (EPMA) CAMECA SXFive instrument at DST-SERB National Facility, Department of Geology (Center of Advanced Study), Institute of Science, Banaras Hindu University. The CAMECA SXFive instrument was operated by SXFive Software at a voltage of 15 kV and current 10 nA with a LaB6 source in the electron gun for the generation of the electron beam. The representative microprobe analyses of various minerals are listed in Table 1. Mineral abbreviations are taken from Whitney & Evans (2010).

Cordierite is more magnesian than coexisting phases (X_{Mg}= 0.769-0.796). No significant compositional zoning was noted in these cordierites. CaO and K_2O are below the detection limit. The X_{Mg} of orthopyroxene in the studied rocks ranges from 0.735 to 0.751 with an alumina content up to 3.752 wt%. Texturally, two orthopyroxene generations can be distinguished on the scale of a thin section. Biotite in the studied rocks is relatively magnesian-rich (X_{Mg} = 0.758-0.767). Its TiO_2 contents are high, ranging from 4.016 to 4.959 wt%. Sapphirine is highly aluminous (up to 62.210 wt% Al_2O_3) and fairly Mg-rich (up to 16.634 wt% MgO). The X_{Mg} varies from 0.774- 0.786. Plagioclase and K-feldspar are dominant in quartzo-feldspathic domains of sapphirine- bearing granulites. X_{Ca} [Ca/(Ca+K+Na)] in plagioclase ranges between 0.416 to 0.421. In alkali feldspar, X_K ranges from 0.014- 0.019. Magnetite, apatite, rutile and zircon present as minor constituents. Small grained zircon inclusions within cordierite show pleochroic haloes.

Phase Equilibria Calculation and Metamorphic Condition(s)

Calculation of the pressure and temperature conditions corresponding to the stability of the preserved mineral assemblages could be achieved by interpretation of the mineral reactions over pressure-temperature petrogenetic grids. P – T pseudosections while constraining the bulk composition of the rock to portray the metamorphic history by confining the mineral assemblage stability fields either between zero-mode isopleths or between univariant reaction lines. The bulk chemical composition has been obtained from the whole rock analysis carried out by XRF facility at the Birbal Sahni Institite of Palaeosciences, Lucknow, Uttar Pradesh, India. The weight% of the major oxides obtained from the analysis was used to draw the phase diagram. The phase diagram was computed using Perple_X 6.8.7 software by freely minimizing the thermodynamic energy (Connolly, 1990, 2005, 2009; Connolly and Petrini, 2002) using the thermodynamic data of Holland and Powell, 1998 and 2001. While computation of minor element, activities such as Mn and Cr were ignored and the calculations were done based on model NCKFMASHT ($Na_2O - CaO - K_2O - FeO - MgO - Al_2O_3 - SiO_2 - H_2O - TiO_2$). The solution models (details in solut_08.dat; Perple_X 6.8.7; database: hp02ver.dat) adopted are Pl (JH), Bi (W), Sapp, Crd (W), Kf, Opx (W), Ilm (W) and melt (W) (Table 2). The amount of H_2O used for P-T pseudosection calculations was approximated by the 'loss on ignition' (LOI) value in the bulk analysis. The P – T figures were obtained through X_{Mg} {Mg / (Fe + Mg)} isopleths of orthopyroxene,

Table 1. Representative microprobe analyses of Sapphirine Granulite

Sample no.	K16	K16	K16	K16	K16	K16	K16	K16	K16	K16	K16	K16	K16	K16	K16
Spot No.	C	S	S	C	S	C	S	R	C	R	C	C	C	C	R
	Spr	Spr	Spr	Opx	Opx	Opx	Crd	Crd	Crd	Bt	Bt	Bt	Kf	Kf	Kf
Oxide wt%															
SiO_2	12.730	13.054	12.982	54.403	53.505	52.790	12.869	13.045	12.577	38.058	37.752	37.887	58.400	58.020	58.761
TiO_2	0.091	0.768	0.730	0.038	0.000	0.056	0.710	0.730	0.635	4.338	4.959	4.016	0.019	0.039	0.078
Al_2O_3	62.210	60.857	60.461	1.976	3.254	3.752	60.320	60.144	60.150	14.401	14.705	15.209	25.795	24.603	24.387
Cr_2O_3	0.180	0.038	0.001	0.022	0.059	0.087	0.054	0.044	0.080	0.183	0.172	0.188	0.005	0.020	0.048
FeO	7.920	8.516	8.420	16.010	16.429	15.986	8.692	8.552	7.799	9.304	9.550	9.823	0.000	0.026	0.078
MnO	0.080	0.025	0.073	0.024	0.178	0.107	0.025	0.110	0.110	0.024	0.012	0.109	0.085	0.000	0.012
MgO	16.310	16.634	16.222	27.099	26.063	26.943	16.241	16.450	17.130	17.138	17.039	17.283	0.222	0.188	0.205
CaO	0.040	0.065	0.044	0.102	0.155	0.112	0.042	0.052	0.031	0.072	0.051	0.024	8.407	8.322	7.929
Na_2O	0.010	0.001	0.031	0.026	0.057	0.044	0.013	0.026	0.003	0.113	0.080	0.073	6.838	7.007	7.096
K_2O	0.030	0.056	0.053	0.009	0.025	0.005	0.063	0.063	0.067	8.864	9.113	8.961	0.265	0.278	0.242
Total	**99.601**	**100.013**	**99.018**	**99.941**	**99.927**	**100.301**	**99.029**	**99.215**	**98.576**	**93.618**	**93.432**	**93.572**	**100.031**	**98.529**	**98.722**
O	10.000	10.000	10.000	4.000	4.000	4.000	18.000	18.000	18.000	22.000	22.000	22.000	8.000	8.000	8.000
Si	0.763	0.782	0.785	1.963	1.936	1.906	1.403	1.419	1.374	5.676	5.593	5.601	2.615	2.652	2.677
Ti	0.004	0.035	0.033	0.001	0.000	0.002	0.058	0.060	0.052	0.487	0.553	0.447	0.001	0.001	0.003
Al	4.394	4.297	4.310	0.084	0.139	0.160	7.751	7.712	7.745	2.531	2.567	2.650	1.362	1.325	1.309
Cr	0.009	0.002	0.000	0.001	0.002	0.002	0.005	0.004	0.007	0.022	0.020	0.022	0.000	0.001	0.002
Fe	0.397	0.427	0.426	0.483	0.497	0.483	0.792	0.778	0.713	1.160	1.183	1.214	0.000	0.001	0.003
Mn	0.004	0.001	0.004	0.001	0.005	0.003	0.002	0.010	0.010	0.003	0.002	0.014	0.003	0.000	0.000
Mg	1.457	1.485	1.462	1.457	1.406	1.450	2.639	2.667	2.789	3.811	3.763	3.809	0.015	0.013	0.014
Ca	0.003	0.004	0.003	0.004	0.006	0.004	0.005	0.006	0.004	0.011	0.008	0.004	0.403	0.408	0.387
Na	0.001	0.000	0.004	0.002	0.004	0.003	0.003	0.005	0.001	0.033	0.023	0.021	0.594	0.621	0.627
K	0.002	0.004	0.004	0.000	0.001	0.000	0.009	0.009	0.009	1.686	1.722	1.690	0.015	0.016	0.014
$\mathbf{X_{Mg}/X_K/X_{Ca}}$	**0.786**	**0.777**	**0.774**	**0.751**	**0.739**	**0.750**	**0.769**	**0.774**	**0.796**	**0.767**	**0.761**	**0.758**	**0.019**	**0.016**	**0.014**

X_{Mg}=Mg/(Mg+Fe^{2+}), X_K=K/(K+ Na+ Ca),X_{Ca}= Ca/(Ca+ Na+ K); * Total iron as FeO; C=Core, R=Rim, S=Symplectite.

cordierite, biotite and sapphirine. Based on the calculated isopleths in correlation with the mineral chemistry data of the studied mineral assemblages, a P – T path was drawn. The P – T path derived shows a retrograde isothermal decompression and a clock-wise P – T trajectory with peak temperature and pressure conditions stable at nearly 985° C and nearly 10 Kbar (Fig. 4) respectively. However, the decompression pressure and temperature conditions as per the modelled isopleths seem to be localised somewhere at or near 7 Kbar and 870 °C respectively (Fig. 4). Such metamorphic conditions are in very much comprehension with the substantial growth of cordierite at the expense of late-stage sapphirine breakdown.

DISCUSSION, COMPARISON AND CONCLUSION

Suranganar sapphirine though more in magnesian still show aluminous ingression. However, during the study no such mineral parageneses could be accounted for high alumina concentration and so a logical explanation that could be reviewed in this context could be an alumina source (such as Sillimanite; R – 1 and R – 2) which got completely consumed during metamorphism. The other way out could be the infiltration of Al – rich melt forming sapphirine – cordierite symplectites on reaction with orthopyroxene (R – 3). The sapphirine chemical composition in the (MgO + FeO) – Al_2O_3 – SiO_2 diagram (Fig. 5) plot between 7:9:3 and 2:2:1. The X_{Mg} variance is slight in the studied sapphirine and ranges from 0.774 to 0.786 which is lower (Anto - X_{Mg}: 0.87 – 0.91 and Shazia - X_{Mg}: 0.885 – 0.897) in comparison to the previous studies done by Anto et. al., 1997 and Shazia et al., 2012 in the nearby area. Also, Eastern Kodaikanal ranges record X_{Mg} range of 0.73 to 0.87 which is still slightly higher than the studied sapphirine from the Suranganar.

The mineral parageneses recorded by Anto et al. (1997) show the presence of spinel and the sapphrine and the Shazia et al. (2012) studies show peraluminous nature. On the contrary, the Suranganar sapphirine bearing rock neither has spinel nor the sapphirine shows peraluminous concentration as from the aforementioned studies. However, the Mg concentration in all the three sapphirines is higher and they all lack the presence of any Al – bearing phase as well as the rock is devoid of garnet and quartz.

The uniqueness of the granulites from the studied area lies in the

Table 2. Solution notation, formula and model sources for phase diagram calculation

Symbol in Perple_X solution model file	Symbol	Solution Name	Formula	Source
Opx (W)	Opx	Orthopyroxene	$[Mg_xFe_{1-x}]_{2-y}Al_{2y}Si_{2-y}O_6$	White et al. (2014)
Bi (W)	Bio	Biotite	$K[Mg_xFe_yMn_{1-x-y}]_{3-u-v-w}Fe_{3+w}Ti_uA_{l1}+vSi_{3-v}O_{10}(OH)_{2-2u}$, $x+y\leq1$, $u+v+w\leq1$	White et al. (2014)
Crd (W)	Crd	Cordierite	$Mg_{2x}Fe_{2}yMn_2(1–x–y)Al_4Si_5O_{18}\bullet(H_2O)_z$, $x+y\leq1$	White et al. (2014)
Melt (W)	melt	melt	Na-Mg-Al-Si-K-Ca-Fe hydrous silicate melt	White et al. (2014)
Sapp	Sap	Sapphirine	$[Mg_xFe_{1-x}]_{4-y/2}Al_{9-y}Si_{2-y/2}O_{20}$	Ideal
Pl(JH)	Pl	Plagioclase	$K_yNa_xCa_{1-x-y}Al_{2-x-y}Si_{2+x+y}O_8$, x + y ≤ 1	Jennings & Holland (2015)
Ilm (W)	Ilm	Ilmenite	$Mg_xMn_yFe_{1-x-y}TiO_3$, x+y ≤ 1	White et al. (2014)

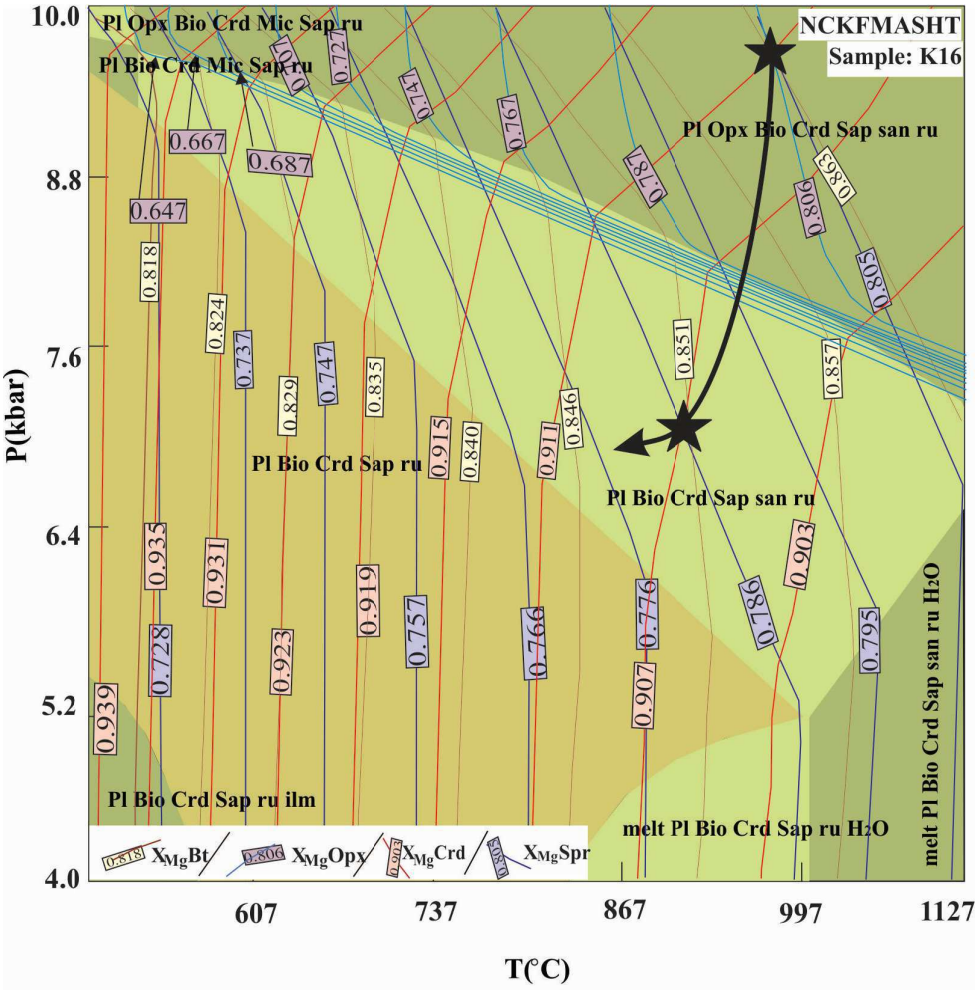

Fig.4. (a) P-T pseudosection calculated for the sapphirine granulite (sample no. K16) in the model system Na_2O-CaO-K_2O–FeO–MgO–Al_2O_3–SiO_2–H_2O-TiO_2 (NCKFMASHT). Bulk composition in weight % (Na_2O-0.69, SiO_2-45.38, Al_2O_3-31.75, FeO-2.93, MgO-12.00, CaO-1.96, K_2O-2.21, H_2O- 1.79, TiO_2- 0.69). The inferred isothermal decompressional P–T path is shown by the arrow. Distribution of the calculated composition isopleths of different minerals for the calculated pseudosection: X_{Mg} biotite, X_{Mg} orthopyroxene, X_{Mg} sapphirine and X_{Mg} cordierite.

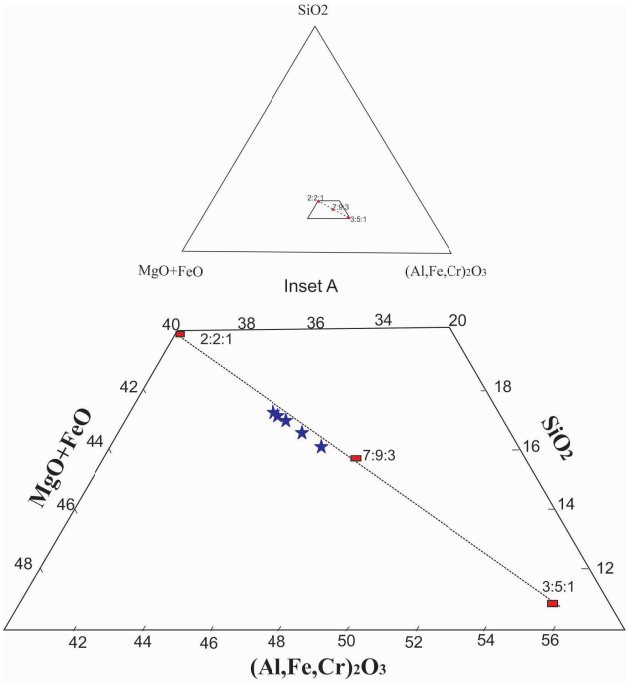

Fig.5. (MgO+FeO)-$(Al,Fe,Cr)_2O_3$-SiO_2 diagram showing the composition plots of sapphirines which falls between 7:9:3 and 2:2:1.

enrichment of Mg in orthopyroxene in these Mg – Al granulites which is different from other granulites present in and around the Madurai block. However, besides this uniqueness one of the important concept to be understood is the source of heat that caused high to ultra-high temperature metamorphism. To achieve this goal a detailed petrological and isotopic investigations are required to understand about the deep crustal tectono – metamorphic evolution.

Acknowledgement: This work has been possible through DST (SERB) research project (P-07-704) to DP and JRF (UGC) to SKR. The authors thank anonymous reviewers for constructive comments that led to substantial improvement in the manuscript.

References

Anto, F.K., Janardhan, A.S. and Shivasubramanian, P. (1998) A new sapphirine occurrence from Kambam valley, Tamil Nadu and its possible relation to the Pan-African tectonothermal event. Curr. Sci., v.73, pp.792–796.

Benisek, A., Dachs, E. and Kroll, H. (2010) A ternary feldspar-mixing model based on calorimetric data: development and application. Contrib. Mineral. Petrol., v.160, pp. 327-337.

Connolly, J.A.D. (2009) The geodynamic equation of state: what and how. Geochem., Geophys., Geosyst., v.10, pp.Q10014.

Connolly, J.A.D. (2005) Computation of phase equilibria by linear programming: a tool for geodynamic modelling and its application to subduction zone decarbonation. Earth Planet. Sci. Lett., v.236, pp.524–541.

Connolly, J.A.D. (1990) Multivariable phase-diagrams-an algorithm based on generalized thermodynamics. Amer. Jour. Sci., v.290, pp.666-718.

Connolly, J.A.D. and Petrini, K. (2002) An automated strategy for calculation of phase diagram sections and retrieval of rock properties as a function of physical conditions. Jour. Metamorp. Geol., v.20, pp.697-708.

Deer, W.A., Howie, R.A. and Zussman, J. (1978) Rock-forming minerals, (2nd edition), single-chain silicates, v.2A, pp.614-639.

Grew, E.S. (1984) Note on sapphirine and sillimanite+ orthopyroxene from Panrimalai, Madurai district, Tamil Nadu. Jour. Geol. Soc. India, v.25(2), pp.116-119.

Harley, S. L., Hensen, B. J., and Sheraton, J. W. (1990) Two stage decompression in orthopyroxene–sillimanite granulites from Forefinger Point, Enderby Land, Antarctica: implications for the evolution of the Archaean Napier Complex. Jour. Metamorp. Geol., v.8(6), pp.591-613.

Holland, T.J.B. and Powell, R. (2001) Calculation of phase relations involving haplogranitic melts using an internally consistent thermodynamic dataset. Jour. Petrol., v.42, pp.673–683.

Holland, T.J.B. and Powell, R. (1998) An internally consistent thermodynamic data set for phases of petrological interest. Jour, Metamorp. Geol., v.16, pp.309–343.

Jennings E. S. and Holland T. J. B. (2015) A simple thermodynamic model formelting of peridotite in the system NCFMASOCr. Jour. Petrol., v.56, pp.869–92.

Kelsey, D.E. (2008) On ultrahigh-temperature crustal metamorphism. Gondwana Res., v.13(1), pp.1-29.

Kelsey, D.E., and Hand, M. (2015) On ultrahigh temperature crustal metamorphism: phase equilibria, trace element thermometry, bulk composition, heat sources, timescales and tectonic settings. Geoscience Frontiers, v.6(3), pp.311-356.

Moore, P. B. (1968) Crystal structure of sapphirine. Nature, v.218, pp.81 – 82.

Mukhopadhyay, D., and Basak, K. (2009) The Eastern Ghats Belt: A polycyclic granulite terrain. Jour. Geol. Soc. India, v.73(4), pp.489-518.

Prakash, D., Vishal, B., Naik, A.S., Yadav, R., Rai, S.K., Tewari, S., Yadav, M.K., Tiwari, S., Dash, S. and Pattnaik, C. (2019) New Occurrence of Sapphirine-spinel-bearing Granulite from NW of Chilka Lake, Eastern Ghats Belt, Odisha. Jour. Geol. Soc. India, v.93, pp.153 – 156.

Prakash, D. Yadav, R. Tewari, S. Frimmel, H. E. Koglin, N. Sachan, H. K. and Yadav, M. K. (2018) Geochronology and phase equilibria modelling of ultra-high temperature sapphirine+ quartz bearing granulite at Usilampatti, Madurai Block, Southern India. Geol. Jour., v.53, pp.139-158.

Raith, M., Karmakar, S. and Brown, M. (1997) Ultrahigh-temperature metamorphism and multi-stage decompressional evolution of sapphirine granulites from the Palni hill ranges, southern India. - Jour. Metamorp. Geol., v.15, pp.379–399.

Sajeev, K., Santosh, M. and Kim, H.S. (2006) Partial melting and P–T evolution of the Kodaikanal metapelite belt, southern India. Lithos, v.92, pp.465–483.

Santosh, M., Xiao, W.J., Tsunogae, T., Chetty, T.R.K. and Yallappa, T. (2011) The neoproterozoic subduction complex in southern India: SIMS zircon U–Pb ages and implications for Gondwana assembly. Precambrian Res., v.192, pp.190–208.

Santosh, M., Maruyama, S. and Sato, K. (2009) Anatomy of a Cambrian suture in Gondwana: Pacific-type orogeny in southern India? Gondwana Res., v.16, pp.321–341.

Santosh, M., and Sajeev, K. (2006) Anticlockwise evolution of ultrahigh-temperature granulites within continental collision zone in southern India. Lithos, v.92(3-4), pp.447-464.

Santosh, M., Yokoyama, K., Biju-Sekhar, S. and Rogers, J.J.W. (2003) Multiple Tectonothermal events in the granulate blocks of southern India revealed from EPMA dating: implications on the history of supercontinents. Gondwana Res., v.06, pp.29–63.

Shazia, J. R., Santosh, M., and Sajeev, K. (2012) Peraluminous sapphirine–cordierite pods in Mg-rich orthopyroxene granulite from southern India: Implications for lower crustal processes. Jour. Asian Earth Sci., v.58, pp.88-97.

Vogt, T. (1947) Bull. de. la comm. - Geol. De Finlande, v.24(140), 15p.

White, R.W., Powell, R. and Holland T.J.B., Johnson T.E. and Green E.C.R. (2014) New mineral activity–composition relations for thermodynamic calculations in metapelitic systems. Jour. Metamorp. Geol., v.32, pp. 261-286.

Whitney, D. L. and Evans, B. W. (2010) Abbreviations for names of rock-forming minerals. Amer. Mineral., v.95, pp.185-187.

(Received: 7 April 2020; Revised form accepted: 26 November 2020)